

1 Long-lived particle searches with the ILD experiment

2 *Daniel Jeans*², *Jan Franciszek Klamka*^{1,*}, and *Aleksander Filip Żarnecki*¹

3 ¹Faculty of Physics, University of Warsaw, Pasteura 5, 02-093 Warsaw, Poland

4 ²KEK, 1-1 Oho Tsukuba, Ibaraki 305-0801, Japan

5 **Abstract.** Future e^+e^- colliders provide a unique opportunity for long-lived
6 particle (LLP) searches. This study focusses on LLP searches using the In-
7 ternational Large Detector (ILD), a detector concept for a future Higgs fac-
8 tory. The signature considered is a displaced vertex inside the ILD's Time Pro-
9 jection Chamber. We study challenging scenarios involving small mass split-
10 tings between heavy LLP and dark matter, resulting in soft displaced tracks.
11 As an opposite case, we explore light pseudoscalar LLPs decaying to boosted,
12 nearly collinear tracks. Backgrounds from beam-induced processes and physi-
13 cal events are considered. Various tracking system designs and their impact on
14 LLP reconstruction are discussed. Assuming a single displaced vertex signa-
15 ture, model-independent limits on signal production cross section are presented
16 for a range of LLP lifetimes, masses, and mass splittings. The limits can be
17 used for constraining specific models, with more complex displaced vertex sig-
18 natures.

19 1 Introduction

20 Despite the remarkable success of the Standard Model (SM) of particle physics, many
21 phenomena, such as the existence of dark matter, baryon asymmetry, or the origin of neutrino
22 masses, remain unexplained by the theory. However, no direct observation of any physics
23 Beyond the Standard Model (BSM) has been made so far, regardless of numerous searches at
24 the Large Hadron Collider (LHC) or other experiments.

25 An interesting concept that could explain why the new physics evades detection is a po-
26 tential existence of BSM long-lived particles (LLPs). Such states, just like many particles in
27 the SM, could travel macroscopic distances before decaying, making it very challenging to
28 observe them. This idea gained a lot of interest in the last years, as the LLPs can naturally
29 appear in many BSM models and be characterised by a range of very distinct signatures [1].
30 Experiments at the LHC performed a large number of searches for LLPs using many new
31 interesting techniques and signatures. However, the main mechanisms responsible for an
32 enhancement of particle lifetime include reduced couplings to the SM sector or small mass
33 differences in a particle decay chain [2]. This, by definition, makes it very difficult to search
34 for such states in the busy environment of a hadron collider.

35 According to the last 2020 Update of the European Strategy for Particle Physics, an e^+e^-
36 Higgs factory is “the highest-priority next collider” [3]. Currently, there are several propos-
37 als for such a machine, and the most mature concept is The International Linear Collider

*e-mail: jan.klamka@fuw.edu.pl

38 (ILC) [4]. The triggerless operation and clean environment of a linear e^+e^- collider make
 39 it very promising in the context of searches for rare and exotic processes, such as LLP pro-
 40 duction. One of the experiments proposed for operation at a future Higgs factory is the
 41 International Large Detector (ILD) [5]. The ILD baseline design is optimized for event re-
 42 construction with the particle-flow approach [6] based on highly granular calorimeters. The
 43 ILD tracking systems include a pixel vertex detector (VTX) and a silicon inner tracker (SIT),
 44 surrounded by a large time projection chamber (TPC). The TPC allows for almost continuous
 45 tracking, which is an excellent feature in the case of searches for delayed decays. For details
 46 about the ILD see Ref. [5] and references therein. This contribution presents prospects for
 47 detection of neutral LLPs with the ILD, using ILC operating at $\sqrt{s} = 250$ GeV (ILC250) as
 48 a reference collider.

49 2 Analysis strategy and benchmark scenarios

50 The study is conducted from an experiment-oriented point of view. The aim was to test
 51 the ILD sensitivity to LLPs on the basis of its experimental features. Therefore, benchmark
 52 scenarios were not selected as preferred points in the parameter space of a particular BSM
 53 model. Instead, test scenarios involved challenging signatures that allow for testing capa-
 54 bilities and potential limitations of detectors and reconstruction techniques. As a signal of
 55 neutral LLP production, we consider a generic case of two tracks that form a displaced ver-
 56 tex; it is a conservative approach, as the so-called displaced jet signature (with more tracks
 57 in the final state) should be even more clean and easier to detect. No further assumptions are
 58 made about the final state, which allows one to keep the analysis model independent.

59 Two opposite classes of benchmarks are considered. The first one involves production
 60 of a heavy LLP, which leads to a signature of a very soft displaced track pair in the final
 61 state. Events for the analysis were generated in the framework of Inert Doublet Model [7],
 62 using pair-production of neutral heavy scalars, A and H , where the former is the LLP and the
 63 latter is stable (and escapes undetected). The LLP decay channel is $A \rightarrow Z^{(*)}H \rightarrow \mu\mu H$, with
 64 muons chosen to simplify the simulation process. The mass of LLP and the proper decay
 65 length were fixed to $m_A = 75$ GeV and $c\tau = 1$ m, respectively. Four mass splitting values
 66 between A and H were considered: $m_A - m_H = 1, 2, 3, 5$ GeV. The mass of A and the small
 67 mass splitting result in a very low transverse momentum of the final state.

68 The second class features exactly opposite case, i.e. production of a very light and highly
 69 boosted LLP, leading to a strong collimation of the final-state tracks. It was generated using
 70 the associated production of an axion-like particle [8], a pseudoscalar LLP, with a hard photon
 71 ($e^+e^- \rightarrow a\gamma$), again only with $a \rightarrow \mu\mu$ decays. Four masses of LLP were considered, $m_a =$
 72 $0.3, 1, 3, 10$ GeV, with the decay lengths $c\tau = 10 \cdot m_a$ mm/GeV to maintain large number of
 73 decays within the detector volume.

74 The analysis was based on a vertex-finding algorithm designed for the purpose of this
 75 study, which reconstructs the vertex in between the points of closest approach of track hel-
 76 lices, if the distance between the points is smaller than 25 mm. The main assumption was
 77 to consider only the displaced vertex signature in the TPC, ignoring any other activity inside
 78 the detector. This allows one to perform the analysis as an ‘‘anomaly search’’ in a model-
 79 independent way, by looking for any excess in a number of vertices over the SM background.
 80 The study was carried out using full detector response simulation based on GEANT4 [9], with
 81 iLCSoft v02-02-03 [10] used for reconstruction.

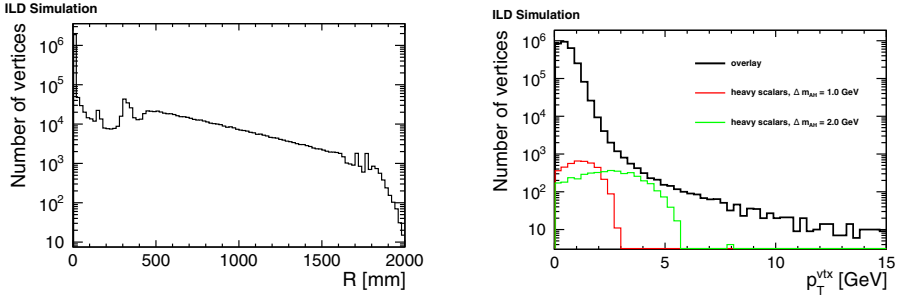


Figure 1: Left: Number of displaced vertices found in the overlay sample as a function of distance from the beam axis. Right: Total transverse momentum of tracks coming from a displaced vertex for the overlay (black) and scalar pair-production with $\Delta m_{AH} = 1$ GeV (red) and $\Delta m_{AH} = 2$ GeV (green). All histograms are normalized to the number of simulated events and correspond to no selection applied at all, just except for the required maximum distance between track helices.

82 3 Background reduction

83 Two types of background have been taken into account – soft, beam-induced (low- p_T)
 84 processes and hard (high- p_T) processes. At linear e^+e^- colliders, due to strong beam focusing,
 85 each bunch crossing (BX) is accompanied by $\gamma\gamma$ collisions, producing low- p_T hadrons
 86 and incoherent e^+e^- pairs. On average, 1.55 hadron photoproduction events and $O(10^5)$ in-
 87 coherent pairs are expected at ILC250 per BX (where most of the latter escape through the
 88 beam pipe and only a small fraction might enter the detector region). These so-called overlay
 89 events are typically analyzed in the context of hard processes (as they can occur in the
 90 detector simultaneously), but in some cases can constitute background on their own.

91 Figure 1 (left) presents a distribution of the vertices reconstructed by the algorithm in
 92 the overlay sample as a function of the distance from the beam axis. It shows there is a huge
 93 number of vertices, in particular close to the beam and to the inner wall of TPC ($R \approx 329$ mm),
 94 most of which are fake. In Fig. 1 the combined p_T^{vx} of tracks forming a vertex in the overlay
 95 events is compared with the signal scenarios in the heavy scalar production case. Taking into
 96 account $O(10^{11})$ BXs expected per year at the ILC, this shows the beam-induced processes
 97 are a significant standalone background, if one wants to consider soft signals.

98 To reject fake vertices, a set of cuts was applied on the variables describing kinematic
 99 properties of tracks, such as their opening angle, number of hits, or a distance between vertex
 100 and a first hit, relative to the track length. The main background sources that remain include
 101 long-lived neutral hadron decays (V^0 particles) and photon conversions, as well as secondary
 102 interactions of particles with the detector material. To suppress the V^0 s, matching with a
 103 dedicated ILC software (processor) for V^0 identification is applied. However, due to a limited
 104 efficiency of the processor, further selection was needed. Invariant mass of a track pair system
 105 was calculated assuming that tracks are either both pions, one is a pion and the other is a
 106 proton, or both are electrons. Then, for the respective track mass hypotheses, vertices formed
 107 by tracks with an invariant mass corresponding to windows of ± 50 MeV around K^0 and Λ^0
 108 masses, and with a mass below 150 MeV (photon conversion) were rejected. Vertices created
 109 by interactions of charged particles with the detector are mitigated by restricting the search
 110 region to vertex radii in the 0.4-1.5 m range and by requirements related to impact parameter
 111 of tracks surrounding and forming the vertex.

Table 1: The vertex finding rates directly obtained for the high- p_T SM backgrounds inside the TPC region after different sets of cuts. Large statistical uncertainties for tight selection rates result from small number of MC events remaining after the selection.

background channel	qq	qqqq	$\gamma^{B/W}\gamma^{B/W}$
Finding rate (standard)	$(7.99 \pm 0.68) \cdot 10^{-4}$	$(1.486 \pm 0.094) \cdot 10^{-3}$	$(2.13 \pm 0.28) \cdot 10^{-5}$
Finding rate (tight)	$(2.30 \pm 1.15) \cdot 10^{-5}$	$(3.57 \pm 1.46) \cdot 10^{-5}$	$(1.06 \pm 0.61) \cdot 10^{-6}$

112 Because it is not possible to generate event samples corresponding to the number of
 113 $O(10^{11})$ BXs expected in the real experiment, factorisation of the final selection was per-
 114 formed. Cuts were applied on variables that are not correlated, using event samples after
 115 the preliminary selection described above. Then, the total reduction factor can be obtained
 116 by multiplication of the individual cut efficiencies on two variables we used. The first was
 117 the total transverse momentum p_T^{tx} of a pair of tracks, since the background is expected to
 118 occupy the region of very low p_T , as visible in Figure 1 (right). The second variable was
 119 a combination of a distance (in three dimensions) between track first hits in the TPC and a
 120 distance between centres of helix-circles (projections of track helices onto the XY plane) of
 121 the tracks. Cuts on these two variables, combined with the preliminary selection efficiency,
 122 give the total reduction factor of $1.26 \cdot 10^{-10}$.

123 The main background sources mentioned above happen predominantly inside the
 124 hadronic jets, therefore, in the case of hard processes we consider background channels with
 125 a hadron production: $q\bar{q}$, $q\bar{q}q\bar{q}$, $qq\ell\nu$, $qq\ell\ell$, $qq\nu\nu$, and a hard $\gamma\gamma$ scattering. As the vertex
 126 finding rates for these backgrounds were found to be dependent on the number of jets, rather
 127 than on the process itself, only the most significant channels ($q\bar{q}$, $q\bar{q}q\bar{q}$, and $\gamma\gamma$) were pro-
 128 cessed to directly obtain the reduction factors, in order to reduce the computational time. To
 129 further reduce background from coincidences of random tracks within high p_T hadronic jets,
 130 a separate cut on a distance between first hits of the tracks was applied in addition to the
 131 selection targeting beam-induced backgrounds described above. This whole set of cuts will
 132 be referred to as the *standard* selection.

133 To improve the background rejection and further reduce vertices from semileptonic K_L^0
 134 decays and to photon conversions with poorly reconstructed, short tracks, we consider also a
 135 *tight* selection. In this case, the cuts on the invariant mass were enhanced, such that vertices
 136 with masses below 700 MeV are rejected for electron and pion track mass hypotheses. In
 137 addition, an isolation criterion was used, since most of the BSM scenarios predict the signal
 138 should be isolated, while vertices in the background samples are found mostly inside hadronic
 139 jets. The resulting vertex finding rates in the simulated background samples are summarized
 140 in Table 1, together with corresponding statistical uncertainties, for both standard and tight
 141 selection.

142 4 Results

143 Figure 2 presents the vertex finding efficiency after standard selection for two of the sig-
 144 nal scenarios, heavy scalar pair-production with $\Delta m_{AH} = 2$ GeV (left) and for the light pseu-
 145 doscalar production with $m_a = 1$ GeV (right). The efficiency is shown as a function of a true
 146 LLP decay vertex position inside the detector, where a reconstructed vertex was considered
 147 “correct” if it was closer than 30 mm from the true vertex. The cut on the vertex radius was
 148 removed to indicate differences between reconstruction efficiency in the silicon tracker and

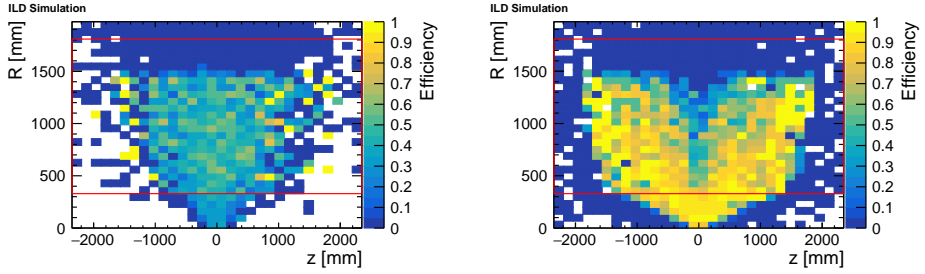


Figure 2: Vertex finding efficiency after the standard selection, but without the cut on the vertex radius, as a function of the true LLP decay vertex position in the detector. The efficiency is shown for the heavy scalar pair-production with $\Delta m_{AH} = 2$ GeV (left) and for the light pseudoscalar production scenario with $m_a = 1$ GeV (right). The TPC volume is shown with the red box.

Table 2: The vertex finding efficiency inside the TPC region obtained in the analysis after different sets of cuts, both for scalars pair-production and light pseudoscalars for all considered scenarios.

Δm_{AH} [GeV]	1	2	3	5
Efficiency (standard) [%]	3	33.2	43.4	51.1
Efficiency (tight) [%]	0.4	28.3	40.7	50.2
m_a [GeV]	0.3	1	3	10
Efficiency (standard) [%]	7.4	48.4	61.7	65.8
Efficiency (tight) [%]	–	47.3	61.7	65.8

149 inside the TPC. It can be noticed that in case of the soft final state, efficiency within the TPC
150 region tend to be slightly higher, which is thanks to large number of hits produced by the
151 tracks. For the vertices with high- p_T tracks the efficiency is higher for decays in the silicon
152 trackers, because these tracks are highly collimated and the silicon trackers provide higher
153 point resolution.

154 Total vertex finding efficiencies, for all signal scenarios considered and both standard
155 and tight selections, are summarized in Table 2. In the case of heavy scalars, the efficiency
156 strongly depends on the Z^* virtuality which determines the final state boost. The sensitivity
157 to $\Delta m_{AH} = 1$ GeV scenario is suppressed by the $p_T^{plx} > 1.9$ GeV cut applied to reduce the
158 background from overlay events, while for the rest of scenarios good sensitivity is achieved.
159 For the light LLP, the efficiency decreases with the final state boost, as opposed to the heavy
160 scalar case. In the $m_a = 300$ MeV scenario most of the vertices are poorly reconstructed due
161 to high colinearity and therefore removed by quality cuts. For tight selection, the sensitivity
162 is completely lost because of cuts on the invariant mass smaller than 700 MeV. It is important
163 to note, that for both $\Delta m_{AH} = 1$ GeV and $m_a = 300$ MeV scenarios the reach could be
164 significantly improved by a dedicated approach, with a selection optimized for each type of
165 scenario (i.e. using information about the missing energy or the hard photon).

166 The vertex finding efficiencies ϵ_{sel} were translated into the expected 95% C.L. limits on
167 the signal production cross section. They were calculated assuming 2 ab^{-1} of the integrated
168 luminosity, the total estimated number of $1.06 \cdot 10^{12}$ of the overlay events and the background
169 rejection factors from Sec. 3. An event re-weighting using the exponential distribution was

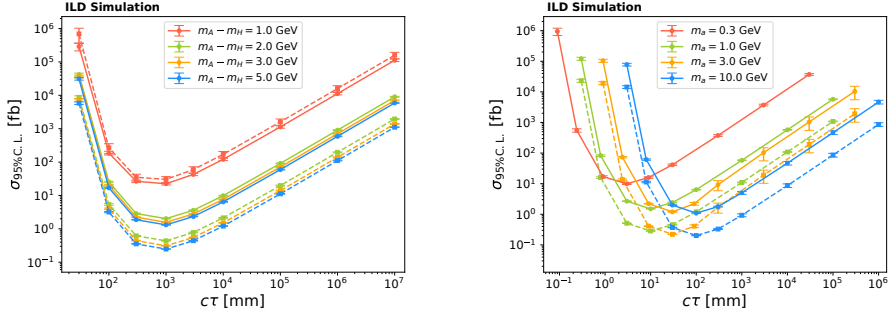


Figure 3: Expected 95% C.L. upper limits on the signal production cross-section for the considered benchmarks and different LLP mean decay lengths, for the scalar pair-production (left) and the light pseudoscalar production (right) at $\sqrt{s} = 250$ GeV. Solid lines corresponds to the standard selection and dashed lines to the tight set of cuts. The uncertainties are statistical.

170 also performed to obtain the limits for a range of LLP lifetimes without generating and pro-
 171 cessing a large number of event samples.

172 The 95% C.L. limits $\sigma_{95\%C.L.}$, corresponding to the number $N_{lim} = 1.96 \sqrt{N_{bg}}/\epsilon_{sel}$, are
 173 presented in Fig. 3 as a function of LLP proper decay length $c\tau$, for both sets of cuts and
 174 all scenarios considered, for the heavy (left) and light (right) LLP production. In case of the
 175 scalar pair-production, limits at the order of femtobarns can be reached in the $c\tau$ range of
 176 0.3-10 m. This can be improved by an order of magnitude with the tight selection for most
 177 of scenarios, except for the most challenging $\Delta m_{AH} = 1$ GeV benchmark, for which the limit
 178 gets slightly worsened because of the enhanced cuts on a track pair invariant mass. For the
 179 light pseudoscalar case, the level of femtobarns is achieved in range of 3-1000 mm of proper
 180 decay lengths. That is again improved by an order of magnitude by the tight selection, except
 181 for the scenario with the smallest mass, for which the sensitivity is completely lost, as in this
 182 case the mass peak is fully below the track pair mass threshold used in the tight selection.

183 5 Impact of the detector design

184 Influence of the detector design on the sensitivity to LLP decays to soft final states has
 185 also been tested. For that purpose, an alternative ILD design was used, in which the TPC
 186 was replaced by an all-silicon outer tracker, taken from the detector model proposed for the
 187 Compact Linear Collider (CLICdet) [11]. One barrel layer had to be added and spacing
 188 between endcap layers increased in order to fit the ILD geometry. For track reconstruction in
 189 the alternative detector model the Conformal Tracking [12] was used, a pattern recognition
 190 algorithm designed originally for CLICdet.

191 Figure 4 presents the track reconstruction efficiency as a function of the true LLP decay
 192 vertex distance from the beam axis, for different scenarios with the heavy scalar production.
 193 The efficiency is compared for the standard and alternative ILD designs. For decays close
 194 to the interaction point, where both detector models are identical, the performance is very
 195 similar. However, for higher displacements, the efficiency drops quickly in the case of the
 196 all-silicon tracker (reaching almost zero already at 1 m), while for the baseline ILD design it
 197 remains high almost throughout the whole detector volume. The reason is a limited number
 198 of layers in the silicon tracker. At least 4 hits are required to reconstruct a track, and the

199 biggest drop in efficiency is visible at the distance of 500 mm, from which only four barrel
 200 layers remain. Also, even having 4 hits does not guarantee reconstruction of a high-quality
 201 track.

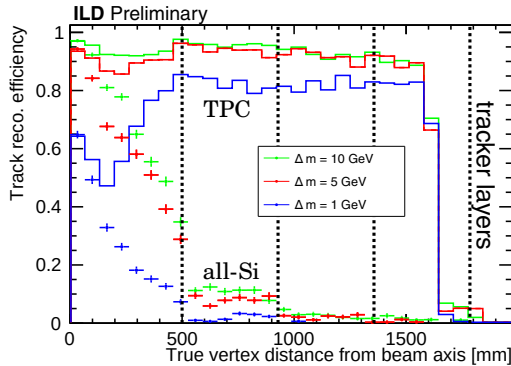


Figure 4: Track reconstruction efficiency as a function of distance from the beam axis for the heavy scalar samples in the all-silicon ILD design (points), compared to efficiency in the baseline TPC-equipped ILD (solid lines). Different colours correspond to particular scalar mass-splitting scenarios in the test samples. Vertical dashed lines show the position of barrel layers of the outer silicon tracker in all-silicon model.

202 6 Conclusion

203 We analyze the prospects for detecting neutral LLPs at the ILD experiment with a dis-
 204 placed vertex signature. An experiment-focused approach was used, in which we select
 205 benchmarks not fully tested at the LHC, based on their kinematic properties. Two very chal-
 206 lenging signatures were studied; the first with a heavy LLP production and a very soft final
 207 state, and the opposite one, with high- p_T , almost colinear tracks originating from a displaced
 208 vertex. We study background sources both from beam-induced, and hard processes.

209 Based on expected background levels and the obtained signal selection efficiencies, we
 210 find that neutral LLP production could be constrained with the ILD down to the level of 0.1 fb
 211 in a wide range of LLP proper decay lengths, 0.003-10 m, depending on the kinematics of the
 212 final state. However, it should be noted that the results are based on a very model-independent
 213 approach and should be considered conservative; a dedicated approach taking into account
 214 particular signal properties would further improve the results.

215 The impact of the detector design on the sensitivity to LLPs was also tested. The re-
 216 sults confirm the expectations that TPC can significantly enhance detector acceptance, and
 217 therefore also the reach for LLP decays to soft final states.

218 Acknowledgements

219 The work was supported by the National Science Centre (Poland) under OPUS research
 220 project no. 2021/43/B/ST2/01778. We would like to thank the LCC generator working group
 221 and the ILD software working group for providing the simulation and reconstruction tools
 222 and producing the Monte Carlo samples used in this study. This work has benefited from
 223 computing services provided by the ILC Virtual Organization, supported by the national re-
 224 source providers of the EGI Federation and the Open Science GRID.

225 **References**

226 [1] J. Alimena et al., Searching for long-lived particles beyond the Standard Model at the
227 Large Hadron Collider, *J. Phys. G* **47**, 090501 (2020), 1903.04497. [10.1088/1361-](https://doi.org/10.1088/1361-6471/ab4574)
228 [6471/ab4574](https://doi.org/10.1088/1361-6471/ab4574)

229 [2] L. Lee et al., Collider Searches for Long-Lived Particles Beyond the Standard Model,
230 *Prog. Part. Nucl. Phys.* **106**, 210 (2019), [Erratum: *Prog.Part.Nucl.Phys.* 122, 103912
231 (2022)]. [10.1016/j.pnpnp.2019.02.006](https://doi.org/10.1016/j.pnpnp.2019.02.006)

232 [3] E.S. Group, 2020 Update of the European Strategy for Particle Physics (CERN Council,
233 Geneva, 2020), ISBN 978-92-9083-575-2

234 [4] P. Bambade et al., The International Linear Collider: A Global Project (2019),
235 1903.01629.

236 [5] H. Abramowicz et al. (ILD Concept Group), International Large Detector: Interim De-
237 sign Report (2020), 2003.01116.

238 [6] M. Thomson, Particle flow calorimetry and the PandoraPFA algorithm, *Nuclear Instru-*
239 *ments and Methods in Physics Research Section A: Accelerators, Spectrometers, De-*
240 *tectors and Associated Equipment* **611**, 25–40 (2009). [10.1016/j.nima.2009.09.009](https://doi.org/10.1016/j.nima.2009.09.009)

241 [7] J. Kalinowski et al., Benchmarking the Inert Doublet Model for e^+e^- colliders, *JHEP*
242 **12**, 081 (2018). [10.1007/JHEP12\(2018\)081](https://doi.org/10.1007/JHEP12(2018)081)

243 [8] R. Schäfer et al., Near or far detectors? A case study for long-lived particle
244 searches at electron-positron colliders, *Phys. Rev. D* **107**, 076022 (2023). [10.1103/Phys-](https://doi.org/10.1103/PhysRevD.107.076022)
245 [RevD.107.076022](https://doi.org/10.1103/PhysRevD.107.076022)

246 [9] S. Agostinelli et al., Geant4 — a simulation toolkit, *Nucl. Instrum. Meth. A* **506**, 250
247 (2003). [https://doi.org/10.1016/S0168-9002\(03\)01368-8](https://doi.org/10.1016/S0168-9002(03)01368-8)

248 [10] ilcsoft – linear collider software, <https://github.com/iLCSoft>

249 [11] N. Alipour Tehrani et al., CLICdet: The post-CDR CLIC detector model (2017).

250 [12] E. Brondolin et al. (CLICdp), Conformal tracking for all-silicon trackers at fu-
251 ture electron–positron colliders, *Nucl. Instrum. Meth. A* **956**, 163304 (2020).
252 [10.1016/j.nima.2019.163304](https://doi.org/10.1016/j.nima.2019.163304)